

# Determination of Activation Energies for Ion Fragmentation by Surface-Induced Dissociation

Samuel B. Wainhaus, Eric A. Gislason, and Luke Hanley\*

Contribution from the Department of Chemistry, m/c 111, University of Illinois at Chicago, Chicago, Illinois 60607-7061

Received July 17, 1996<sup>⊗</sup>

**Abstract:** We describe here a new method for extracting the activation energy for the formation of any fragment or reactively scattered ion that forms from a parent ion–surface collision. Our model is developed from first principles for collision-induced dissociation in the gas phase and then modified for surface-induced dissociation (SID). This approach is conceptually similar to that used for threshold collision-induced dissociation measurements in that it assumes a similar functional form for the dissociation cross section, it takes into account the partitioning of energy between the projectile and the target, and it deconvolutes these over the kinetic energy distribution of the parent ion beam. The activation energy is extracted by an analysis of the energy-resolved mass spectra and the kinetic energy distribution spectra for the surface-scattered ions. We test our method by determining the activation energies for the formation of the  $\text{SiMe}_2^+$ ,  $\text{SiMe}^+$ ,  $\text{SiD}^+$  and  $\text{Si}^+$  fragment ions from the  $d_9\text{-SiMe}_3^+$  parent ion scattered off a hexanethiolate self-assembled monolayer adsorbed on Au(111). The differences between the literature and SID activation energies are rationalized by consideration of the experimental uncertainty in the method.

## I. Introduction

Surface-induced dissociation (SID) has been developed as an alternative to gas-phase collision-induced dissociation (CID) for the fragmentation of polyatomic ions in tandem mass spectrometry.<sup>1–11</sup> The ion–surface collision in SID leads to a transfer of kinetic energy into the internal modes of the ion, causing a fragmentation that can be used for the characterization of the ion. We describe here a new method for extracting the activation energy for the formation of any fragment or reactively scattered ion that forms from a parent ion–surface collision. The activation energy is extracted by an analysis of the energy resolved mass spectrum and the kinetic energy distribution spectra for the surface-scattered ions. We test our method by determining the activation energies for the formation of the  $\text{SiMe}_2^+$ ,  $\text{SiMe}^+$ ,  $\text{SiD}^+$ , and  $\text{Si}^+$  fragment ions from the  $d_9\text{-SiMe}_3^+$  parent ion scattered off a hexanethiolate self-assembled monolayer adsorbed on Au(111).

Low-energy collision-induced dissociation (CID) with noble gas atoms has been successfully applied to the determination of activation or bond dissociation energies for small polyatomic

ions.<sup>12–15</sup> However, SID possesses several characteristics that make it complementary to CID: SID allows the formation of high-energy fragmentation ions not easily produced by low-energy CID,<sup>1,16,17</sup> it deposits a narrower distribution of internal energy into the parent ion,<sup>1–4,18,19</sup> and it is performed in the absence of a collision gas.<sup>5,20</sup> An efficient kinetic to internal energy transfer allows SID to access high-energy fragmentations in a single collision with the surface. In contrast, high-energy fragmentations are either inaccessible to CID or require higher collision energies or multiple collisions from which it is difficult to extract accurate activation energies. For example, reasonable activation energies for  $\text{C}_{60}^+ \rightarrow \text{C}_{58}^+ + \text{C}_2$  have been obtained only by SID.<sup>5,21,22</sup> SID shows particular promise for measuring the activation energies of high-energy fragmentations of biopolymers.

SID may be the preferred method for determining activation energies for higher energy fragmentation channels, but there is little agreement on how to best analyze SID data to obtain those activation energies. One method calculates the transfer of kinetic to internal energy in the parent ion (T–V) for a given ion, then applies this T–V value to other ions. Several strategies have been used to calculate T–V from the energy resolved mass spectrum (ERMS), which is the plot of the normalized SID

\* Address correspondence to this author at the following email address: LHanley@uic.edu.

<sup>⊗</sup> Abstract published in *Advance ACS Abstracts*, April 15, 1997.

(1) Cooks, R. G.; Ast, T.; Mabud, Md. A. *Int. J. Mass Spectrom. Ion Processes* **1990**, *100*, 209 and references therein.

(2) Cooks, R. G.; Ast, T.; Pradeep, T.; Wysocki, V. *Acc. Chem. Res.* **1994**, *27*, 316 and references therein.

(3) Morris, M.; Riederer, D. E., Jr.; Winger, B. E.; Cooks, R. G.; Ast, T.; Chidsey, C. E. D. *Int. J. Mass Spectrom. Ion Processes* **1992**, *122*, 181 and references therein.

(4) Miller, S. A.; Riederer, D. E., Jr.; Cooks, R. G.; Cho, W. R.; Lee, H. W.; Kang, H. *J. Phys. Chem.* **1994**, *98*, 245.

(5) Yerezian, C.; Beck, R. D.; Whetten, R. L. *Int. J. Mass Spectrom. Ion Processes* **1994**, *135*, 79 and references therein.

(6) Somogyi, A.; Kane, T. E.; Ding, J.-M.; Wysocki, V. H. *J. Am. Chem. Soc.* **1993**, *115*, 5275.

(7) Kane, T. E.; Somogyi, A.; Wysocki, V. H. *Org. Mass Spectrom.* **1993**, *28*, 1665.

(8) Dagan, S.; Amirav, A. *J. Am. Soc. Mass Spectrom.* **1993**, *4*, 869.

(9) Burroughs, J. A.; Hanley, L. *Anal. Chem.* **1994**, *66*, 3644.

(10) Wainhaus, S. B.; Burroughs, J. A.; Wu, Q.; Hanley, L. *Anal. Chem.* **1994**, *66*, 1038.

(11) Hayward, M. J.; Park, F. D. S.; Manzella, L. M.; Bernasek, S. L. *Int. J. Mass Spectrom. Ion Processes* **1995**, *148*, 25.

(12) Khan, F. A.; Clemmer, D. E.; Schultz, R. H.; Armentrout, P. B. *J. Phys. Chem.* **1993**, *97*, 7978 and references therein.

(13) Hanley, L.; Ruatta, S. A.; Anderson, S. L. *J. Chem. Phys.* **1987**, *87*, 260.

(14) McLuckey, S. A. *J. Am. Soc. Mass Spectrom.* **1992**, *3*, 599.

(15) Marzluff, E. M.; Campbell, S.; Rodgers, M. T.; Beauchamp, J. L. *J. Am. Chem. Soc.* **1994**, *116*, 7787.

(16) McCormack, A. L.; Somogyi, A.; Dongre, A. R.; Wysocki, V. H. *Anal. Chem.* **1993**, *65*, 2859.

(17) Chorush, R. A.; Little, D. P.; Beu, S. C.; Wood, T. D.; McLafferty, F. W. *Anal. Chem.* **1995**, *67*, 1042.

(18) Williams, E. R.; Henry, K. D.; McLafferty, F. W.; Shabanowitz, J.; Hunt, D. F. *J. Am. Soc. Mass Spectrom.* **1990**, *1*, 413.

(19) Burroughs, J. A.; Wainhaus, S. B.; Hanley, L. *J. Phys. Chem.* **1994**, *98*, 10913.

(20) Williams, E. R.; Jones, G. C., Jr.; Fang, L.; Zare, R. N.; Garrison, B. J.; Brenner, D. W. *J. Am. Chem. Soc.* **1992**, *114*, 3207.

(21) Lill, Th.; Busmann, H.-G.; Lacher, F.; Hertel, I. V. *Chem. Phys.* **1995**, *193*, 199.

(22) Weis, P.; Rockenberger, J.; Beck, R. D.; Kappes, M. M. *J. Chem. Phys.* **1996**, *104*, 3629.

fragment ion signal versus the parent ion kinetic energy.  $T-V$  can be calculated by comparison with known bond energies, but this is obviously useless for determining those bond energies *a priori*.<sup>1-4,6,7,23</sup> Deconvolution of the ERMS with breakdown curves obtained by other techniques has also been successful, but such breakdown curves are unavailable for most ions.<sup>23-25</sup>  $T-V$  typically ranges from 10 to 30% and apparently remains relatively constant for similarly sized ions scattered off a given surface.  $T-V$  also varies with surface composition.<sup>2-7,19,21,23,26</sup> For example,  $T-V$  is larger for fluorocarbon than for hydrocarbon surfaces. Finally, recent work with fullerene ions has shown that  $T-V$  can vary with the size and possibly the shape of the parent ion.<sup>27</sup> We have previously attempted an *a priori* prediction of  $T-V$  using a classical formula which assumes that the collision is impulsive and the masses of all collision partners can be determined.<sup>19,23</sup> However, the accuracy of  $T-V$  obtained by this method is limited by the difficulty of assigning an effective mass to the surface. In general, the accuracy of derived activation energies will be limited for any method that requires the input of an accurate  $T-V$ .

RRK, RRKM, and first-order kinetic decomposition analyses of SID data have also been used to determine activation energies.<sup>5,21,26</sup> One kinetic method determines a first-order Arrhenius constant from thermal dissociation, which is then used to extract activation energies from SID data, although fundamental differences in excitation dynamics argue against a common Arrhenius constant for these two processes.<sup>26</sup> Another kinetic method has obtained the activation energies for  $C_{60}^+$  and  $C_{70}^+$ , but this method utilizes the delayed ionization effect, which has only been observed in fullerenes.<sup>22,27</sup>

We develop here a new method of extracting activation energies from SID measurements of any polyatomic ion. Our model is developed from first principles for CID and then modified for SID. Our approach is conceptually similar to that used for threshold CID measurements in that it assumes a similar functional form for the dissociation cross section, it takes into account the partitioning of energy between the projectile and the target, and it deconvolutes these over the kinetic energy distribution of the parent ion beam. While our model does require an initial guess of the  $T-V$ , the final accuracy of our results can be improved by iteratively refining this guess. We quantitatively determine the energy transfer to the surface by measuring the kinetic energies distribution spectra (KEDS) of the scattered ions. We extract fragmentation energies by a nonlinear least-squares fit of the experimental ERMS with the ERMS predicted by our model. The model is then tested by determining the activation energies for the various fragment ions formed from  $d_9$ -SiMe<sub>3</sub><sup>+</sup> SID at a saturated hexanethiolate self-assembled monolayer adsorbed on a Au(111) surface.

## II. Experimental Section

The experimental setup is only slightly different from that described previously.<sup>28</sup> The only major modification to the experiment was the installation of a quadrupole mass spectrometer (QMS) for primary ion selection. Degassed tetramethylsilane-*d*<sub>12</sub> (D 98%, Cambridge Isotope) was introduced into a 70-eV electron impact ion source to form SiMe<sub>3</sub><sup>+</sup>.

(23) Burroughs, J. A.; Wainhaus, S. B.; Hanley, L. *J. Chem. Phys.* **1995**, *103*, 6706.

(24) Vekey, K.; Somogyi, A.; Wysocki, V. H. *J. Mass Spectrom.* **1995**, *30*, 212.

(25) de Maaijer-Gielbert, J.; Beijersbergen, J. H. M.; Kistemaker, P. G.; Weeding, T. L. *Int. J. Mass Spectrom. Ion Processes* **1996**, *153*, 119.

(26) Meot-Ner, M.; Dongre, A. R.; Somogyi, A.; Wysocki, V. H. *Rapid Commun. Mass Spectrom.* **1995**, *9*, 829.

(27) Beck, R. D.; Rockenberger, J.; Weis, P.; Kappes, M. M. *J. Chem. Phys.* **1996**, *104*, 3638.

(28) Wu, Q.; Hanley, L. *J. Phys. Chem.* **1993**, *97*, 2677.

The 10–70 eV SiMe<sub>3</sub><sup>+</sup> ion beams were directed onto the surface at an incident angle of 45° off normal. The surface was held at 300 K during all ion scattering experiments. The ion beam current varied with ion energy but was generally in the range of 2–7 nA/cm<sup>2</sup>. The SiMe<sub>3</sub><sup>+</sup> (*m/z* 82) typically had impurities of ~8% <sup>29</sup>Si(CD<sub>3</sub>)<sub>3</sub><sup>+</sup> and Si(<sup>13</sup>CD<sub>3</sub>)<sub>3</sub><sup>+</sup> (*m/z* 83) and ~1% each of SiMeD<sub>2</sub><sup>+</sup> (*m/z* 50) and SiMe<sub>3</sub>D<sup>+</sup> (*m/z* 84).<sup>29</sup>

Ion beam currents and energies were measured with a Faraday cup equipped with a three grid retarding field energy analyzer, where the outer grids were at fixed voltages and the central grid voltage was swept at the retarding potential.<sup>28</sup> By taking the first derivative of the ion beam energy distributions, the fwhm of the ion beam was found to be 2–4 eV. It is well-documented that three-grid retarding field energy analyzers tend to overestimate or slightly shift the width and absolute value of the ion energy distributions.<sup>30</sup> This leads us to conclude that the actual fwhm of the incident ion beam may be significantly less than 2–4 eV, although to be conservative, we have used the measured values in our data analyses. The relative agreement between the ion source voltage which defines the ion energy and the retarding field analyzer values, allows us to estimate that the quoted absolute incident ion energies are only accurate to within ±1 eV. This error is due to both the aforementioned measurement inaccuracies and ion source space charge effects.

The main chamber houses a QMS equipped with a Bessel box energy analyzer set to collect positive ions scattered off the surface with energies up to 19 eV at 90° with respect to the incident ion beam. The Bessel box energy window was reduced to 4.5 eV when used to measure the kinetic energy distribution spectra. No attempt was made to detect negative ions or neutrals in these experiments. The background pressure in the main chamber was typically  $8 \times 10^{-10}$  Torr during ion scattering.

A 10-mm-diameter Au(111) single crystal (Monocrystals, Cleveland, OH) was clamped in a homemade tantalum holder and attached to a liquid nitrogen cooled manipulator capable of full xyz movement and rotation. The crystal was initially cleaned by exposure to oxygen at 1000 K followed by repetitive sputter–anneal cycles.<sup>31,32</sup> Low-energy electron diffraction was used to confirm surface cleanliness and order with the appearance of a sharp (1 × 1) pattern. On successive days the crystal was cleaned by repetitive sputter–anneal cycles. A saturated hexanethiolate self-assembled monolayer (C<sub>6</sub>) was prepared by heating the Au(111) crystal to 350 K and dosing with several thousand Langmuir of degassed hexanethiol (Aldrich, 95%). The C<sub>6</sub> surface coverage was monitored by the infrared reflection absorption spectroscopy peak intensity of the C–H stretch.<sup>9,10,33</sup> Both the infrared spectra and the kinetic energy distribution spectra for the scattered ions indicated that we prepared the C<sub>6</sub>/Au(111) at a high coverage where the carbon chains are predominantly standing up on the surface: these points are detailed in a separate paper that compares SID of SiMe<sub>3</sub><sup>+</sup> scattered off clean and C<sub>6</sub> covered Au(111).<sup>33</sup>

All data were reproduced on at least two separate days under identical experimental conditions. The kinetic energy distribution spectra (KEDS) were subjected to second-order fast Fourier transform smoothing to reduce statistical noise.

## III. Theory

A well-studied process in the gas phase is the collision-induced dissociation (CID) of a polyatomic ion in a single collision with a rare gas atom such as Xe. The functional form of the CID cross section  $\sigma$  that is used to analyze the experiments near threshold is

$$\sigma = \sigma_0(E_R - A)^n/E_R \quad (1)$$

(29) Basner, R.; Foest, R.; Schmidt, M.; Sigener, F.; Kurunczi, P.; Becker, K.; Deutsch, H. *Int. J. Mass Spectrom. Ion Processes* **1996**, *153*, 65.

(30) O'Connor, P. J.; Leroi, G. E.; Allison, J. *J. Am. Soc. Mass Spectrom.* **1991**, *2*, 322.

(31) Chesters, M. A.; Somorjai, G. A. *Surf. Sci.* **1975**, *52*, 21.

(32) Besocke, K.; Krahl-Urban, B.; Wagner, H. *Surf. Sci.* **1977**, *68*, 39.

(33) Wainhaus, S. B.; Lim, H.; Schultz, D. G.; Hanley, L. *J. Chem. Phys.* In press.

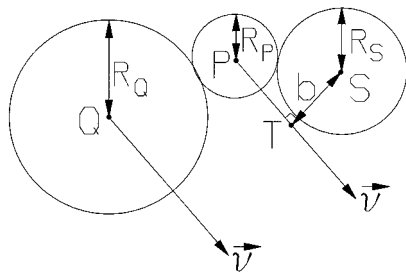


**Figure 1.** The instant of collision between atom S and atom P of the “diatomic” PQ. Before the collision, S is stationary and PQ has velocity  $\bar{v}$ . The S–P atom–atom impact parameter  $b$  is given by the S–T distance.

where  $\sigma_0$  is a scaling constant that includes the maximum cross section,  $E_R$  is the relative collision energy,  $A$  is the threshold or activation energy for dissociation of the ion, and  $n$  is a fitting constant that is generally between 1 and 2.

Our goal is to derive an equivalent expression for surface-induced dissociation (SID). However, there are a number of complications. First, the conversion of the collision energy from the lab frame to the center-of-mass frame is unique in the gas phase because the total energy and momenta of the two colliding particles are known. This is not the case in SID. Some amount of the initial translational energy of the ion is converted into energy of the surface, but this cannot be predicted from a simple conservation of momentum argument. In addition, we would like to be able to derive an expression that can be used over a wider energy range than is typically the case for eq 1.

Our derivation proceeds in several steps. The first step follows a procedure we developed in an earlier paper.<sup>34</sup> We begin by assuming for simplicity that the incoming ion is a diatomic PQ that collides with a single surface atom S of infinite mass. Figure 1 shows PQ colliding with S, along with the relevant parameters for the collision. We also assume that S, P, and Q are hard spheres with radii  $R_S$ ,  $R_P$ , and  $R_Q$  and that initially P and Q are touching, as indicated by Figure 1. If atom P hits S, the maximum energy that can be transferred into PQ,  $E_t$ , as a result of the collision is given by the projection of the lab kinetic energy  $E$  (since S is infinitely heavy,  $E = E_R$ ) along the S–P line of centers; that is, by

$$E_t = E[1 - b^2/(R_S + R_P)^2] \quad (2)$$

Here  $b$  is the S–P atom–atom impact parameter, and  $0 \leq b \leq R_S + R_P$ . The largest value of  $E_t$  ( $E_t = E$ ) comes from  $b = 0$ , and the smallest value ( $E_t = 0$ ) from  $b = R_S + R_P$ . Larger impact parameters are not considered since P does not hit S for  $b \geq R_S + R_P$ , so  $E_t = 0$ . The distribution of  $b$  values is given by

$$P(b) db = 2b db/(R_S + R_P)^2 \quad (3)$$

and it is straightforward to derive the distribution of  $E_t$  at a given  $E$  value:

$$\begin{aligned} P(E_t; E) &= P[b(E_t)] \left| \frac{db}{dE_t} \right| \\ &= 1/E \end{aligned} \quad (4)$$

over the range  $0 \leq E_t \leq E$ . This distribution is very broad, is a constant, and does not depend on the masses or sizes of P and Q. Thus, the model is still valid whether a single or a large portion of the incident projectile PQ recoils during collision with the target S.

In the second step of the derivation we argue that eq 4 will also hold for the collision of an arbitrary polyatomic ion colliding with an infinitely heavy atom S, provided that S collides with a single moiety of the polyatomic. One possible complication with a bulky polyatomic ion, however, is that in some collisions the S–P impact parameter  $b$  may not be able to reach  $(R_S + R_P)$  because some other moiety in the polyatomic hits S first. This would reduce the distribution  $P(E_t; E)$  at small values of  $E_t$ , but SID near threshold is dominated by  $E_t$  values near  $E$ , so that is not a problem.

In the gas phase it is sometimes the case that in the collision of a polyatomic with a rare gas atom at a relative energy  $E_R$  it is not possible to convert the entire energy  $E_R$  into internal excitation of the polyatomic. A good example of this is shown in the recent paper by Hase and co-workers.<sup>35</sup> They used quasiclassical trajectories to study the collisions of the  $\text{Al}_6$  cluster with Ar, and they determined that in most cases the maximum excitation was about 90% of  $E_R$ . They attributed this to the inefficiency of single Ar–Al collisions, and found that the maximum energy transfer could be estimated from the masses of the atoms involved. We believe that the collision of a polyatomic ion with a surface is different, however, since the surface atom S cannot recoil cleanly away from the incoming polyatomic ion. Therefore, we expect that the upper limit for  $E_t$  will always be  $E$  so that eq 4 will be a good approximation to  $P(E_t; E)$ . We take into consideration below the energy transferred to the surface atom S by the collision.

The next step in the derivation is to consider the fate of an ion with internal energy  $E_t$  in excess of the threshold for dissociation  $A$ . In most cases we expect polyatomic ions with  $E_t > A$  to dissociate. However, this need not be true. For example, if the dissociation process occurs while atoms P and S are in contact, it is possible that the threshold for SID depends upon the S–P–Q angle, and molecules with  $E_t > A$  but in an unfavorable configuration cannot dissociate. This type of behavior is commonly seen in reactive scattering.<sup>34</sup> It is also possible that a large polyatomic ion may have enough internal energy to dissociate but does not do so before it reaches the detector. (This is the delayed dissociation or unimolecular decay problem.) Even if the polyatomic ion does dissociate, it may produce a number of possible dissociation products. For example, in our study of  $d_9\text{-SiMe}_3^+$  we see five product ions in addition to the parent ion. With this discussion in mind we define  $p_i(E_t)$  as the fraction of molecules with internal energy  $E_t$  that dissociates to product channel  $i$  before reaching the detector. (The set of  $p_i(E_t)$  for all dissociation products are the breakdown curves that are typically measured in TPEPICO experiments.) The measured SID fraction of products in channel  $i$  at energy  $E$ , denoted  $f_i(E)$ , is then the convolution of  $P(E_t; E)$  in eq 4 with  $p_i(E_t)$ ; that is,

$$\begin{aligned} f_i(E) &= \int_0^E P(E_t; E) p_i(E_t) dE_t \\ &= \frac{1}{E} \int_0^E p_i(E_t) dE_t \end{aligned} \quad (5)$$

We are particularly interested in the behavior of  $f_i(E)$  near threshold.

The simplest example to consider would be for a single dissociation product where  $p_i(E_t)$  increases linearly with  $E_t$  (the first term in a Taylor series expansion), so

(34) Gislason, E. A.; Sizun, M. *J. Phys. Chem.* **1991**, *95*, 8462.

(35) de Sainte Claire, P.; Peshherbe, G. H.; Hase, W. L. *J. Phys. Chem.* **1995**, *99*, 8147.

$$\begin{aligned}
 p_i(E_t) &= 0 & E_t < A \\
 &= (E_t - A)/B & A \leq E_t < A + B \\
 &= 1 & A + B \leq E_t
 \end{aligned} \quad (6)$$

A corresponds to the threshold or activation energy for dissociation of the ion, as it was similarly defined in eq 1.  $1/B$  corresponds to the slope of the dissociation probability near threshold and is used instead of the scaling constant  $\sigma_0$  given in eq 1. Note that eq 6 can be converted into a step function at  $E_t = A$  by setting  $B = 0$ . Substituting eqs 4 and 6 into eq 5 gives

$$\begin{aligned}
 f_i(E) &= 0 & E < A \\
 &= (E - A)^2/2BE & A \leq E < A + B \\
 &= [E - A - B/2]/E & A + B \leq E
 \end{aligned} \quad (7)$$

These functional forms are well known from models of chemical reaction.<sup>34</sup> Comparing this result with eq 1, we conclude that a quadratic dependence on  $(E - A)$  where  $n = 2$  corresponds to a linear increase of  $p_i(E_t)$  with  $E_t$ . In addition, the value  $n = 1$  corresponds to a step function in  $p_i(E_t)$  (i.e.,  $B = 0$ ). A more general form of eqs 6 and 7 can be obtained by assuming that

$$\begin{aligned}
 p_i(E_t) &= 0 & E_t < A \\
 &= (E_t - A)^{n-1}/B^{n-1} & A \leq E_t < A + B \\
 &= 1 & A + B \leq E_t
 \end{aligned} \quad (8)$$

In that case substitution into eq 5 gives

$$\begin{aligned}
 f_i(E) &= 0 & E < A \\
 &= (E - A)^n/[nB^{n-1}E] & A \leq E < A + B \\
 &= \{E - A - [(n - 1)B/n]\}/E & A + B \leq E
 \end{aligned}$$

A third useful way to write  $p_i(E_t)$  is as a Taylor series expansion about  $E_t = A$ . If

$$p_i(E_t) = \sum_{l=1}^{\infty} \alpha_l (E_t - A)^l \quad (10)$$

then substitution into eq 5 gives

$$f_i(E) = [(E - A)^2/E] \sum_{k=0}^{\infty} \alpha_{k+1} (E - A)^k / (k + 1) \quad (11)$$

We have used both eq 7 and eq 9 in our data analysis in this paper.

The final step in the derivation is to recognize that the surface cannot be represented by a single atom S of infinite mass. In reality, S recoils after the collision with the ion and a certain fraction of the initial kinetic energy  $E$  is converted into energy of the surface,  $E_{\text{surf}}$ . Unfortunately,  $E_{\text{surf}}$  must be measured experimentally or calculated from trajectory calculations, so it is not easily obtained. Nevertheless, for the purpose of this derivation we assume that each polyatomic ion in the beam with kinetic energy  $E$  deposits a fixed amount of energy  $E_{\text{surf}}$  into the surface, and we assume that the function  $E_{\text{surf}}(E)$  is known. This energy is not available for internal excitation of the polyatomic ion, and we conclude that  $E_{\text{surf}}$  can be accounted for simply by subtracting it from the total energy available to the system to dissociate the ion. Thus, the fraction of particles in product state  $i$  actually measured at the detector in an SID experiment when the beam kinetic energy is  $E$  is

$$F_i(E) = f_i[E - E_{\text{surf}}(E)] \quad (12)$$

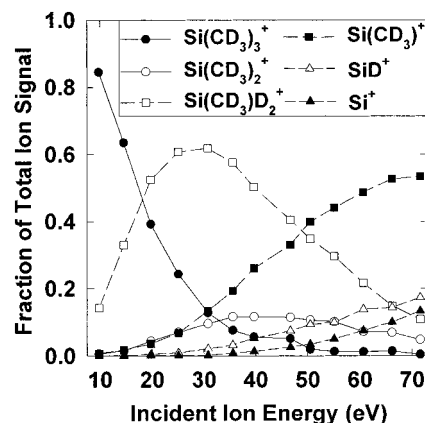


**Figure 2.** Energy resolved mass spectrum (ERMS) of  $d_9$ - $\text{SiMe}_3^+$  scattered off hexanethiolate ( $\text{C}_6$ ) covered Au(111).

where  $f_i$  is defined in eq 5 and the function  $E_{\text{surf}}(E)$  is the energy transferred to the surface, as is discussed further below.

Equation 12 is the final result of the derivation for a fixed beam energy  $E$ . In practice our ion beam has a finite width, and the energy distribution at a nominal beam energy  $E_0$  is well described by

$$P(E; E_0) = (\pi^{1/2} \Delta E)^{-1} \exp[-(E - E_0)^2 / \Delta E^2] \quad (13)$$

The beam width  $\Delta E$  is measured in each experiment (see description of fwhm in the Experimental Section). Consequently, the measured fraction of product  $i$  at the detector for a nominal beam energy  $E_0$  is given by averaging eq 12 over the beam distribution, yielding

$$EF_i(E_0) = \int_0^{\infty} dE_0 P(E; E_0) f_i[E - E_{\text{surf}}(E)] \quad (14)$$

This is the actual expression used in our analysis. The particular functional form of  $f_i$  depends upon the particular product ion and is taken from either eq 7 or eq 9.

#### IV. Results and Data Analysis

**A. Determination of  $E_{\text{surf}}$ .** Our method requires that the energy deposited into the surface,  $E_{\text{surf}}$ , be described as a function of the incident energy of the parent ion  $E$ .  $E_{\text{surf}}$  can be determined experimentally by energy conservation<sup>5</sup> from

$$E = E_{\text{scat}} + E_{\text{int}} + E_{\text{surf}} \quad (15)$$

where  $E_{\text{scat}}$  and  $E_{\text{int}}$  are the kinetic and internal energy, respectively, of the scattered parent ion following the collision event.  $E_{\text{int}}$  is obtained from the plot of the fraction of the total ion signal percentage for each fragment ion versus  $E$  (ERMS), shown for  $\text{SiMe}_3^+$  scattered from  $\text{C}_6/\text{Au}(111)$  in Figure 2. Some of the fragment ions observed in Figure 2 form by sequential methyl loss ( $\text{SiMe}_x^+$ ,  $x = 2-0$ ) while others form via rearrangement ( $\text{SiMe}_2\text{D}_2^+$  and  $\text{SiD}^+$ ).<sup>36</sup>  $E_{\text{scat}}$  is taken as the weighted average of the kinetic energy distribution spectra (KEDS) of scattered  $\text{SiMe}_3^+$  shown in Figure 3. Experimental verification of these  $E_{\text{scat}}$  values comes from the approximate agreement of the scattered parent and fragment ion velocities calculated from the KEDS (fragment ion data not shown).  $E_{\text{int}}$  is determined by deconvoluting the fragment ion fractions given by the ERMS with the literature values for their activation

(36) Groenewold, G. S.; Gross, M. L.; Bursley, M. M.; Jones, P. R. *J. Organomet. Chem.* **1982**, 235, 165.

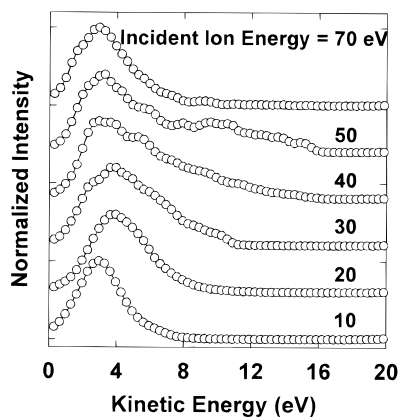


**Figure 3.** Kinetic energy distribution spectra (KEDS) of intact  $d_9$ - $\text{SiMe}_3^+$  ion scattered off  $\text{C}_6/\text{Au}(111)$ . The curves are offset from one another to ease viewing.

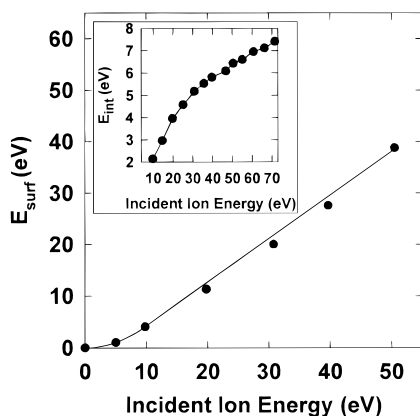


**Figure 4.** Calculated internal energy ( $E_{\text{int}}$ ) and energy transferred to the surface ( $E_{\text{surf}}$ ) for  $d_9$ - $\text{SiMe}_3^+$  scattered off  $\text{C}_6/\text{Au}(111)$ . The points are the values calculated from the data. The curve for  $E_{\text{int}}$  is simply drawn to connect the points, but the curve for  $E_{\text{surf}}$  depicts the function in eq 16.

energies of formation<sup>37</sup> with use of the method of Cooks<sup>23,38</sup>. The internal energy of  $\text{SiMe}_3^+$  as a function of  $E$  is shown in Figure 4.  $E_{\text{surf}}$  is calculated from eq 15 and is plotted as a function of  $E$  as shown in Figure 4. A single linear fit of the  $E_{\text{surf}}$  data results in large deviations and nonphysical behavior below 10 eV. Furthermore, nonlinearity below 10 eV is expected as the collision event shifts from a classical (repulsive region of the potential) to a chemical (attractive region of the potential) scattering regime. We therefore allow for linear behavior above 10 eV, assume quadratic behavior below 10 eV, and insist for mathematical simplicity that the value of  $E_{\text{surf}}$  be zero when  $E$  is zero. While this final assumption may be violated by chemisorption, image charge effects, and/or energy transfer from the initial internal energy of the incoming ion, this likely has little effect upon our results since we are not fitting data at  $E = 0$  eV anyway. Our result is

$$E_{\text{surf}} = kE^2, \quad E < 10 \text{ eV}$$

$$= pE + q, \quad E \geq 10 \text{ eV} \quad (16)$$

where  $k = 0.0433$ ,  $p = 0.846$ , and  $q = -4.22$  for the  $\text{SiMe}_3^+/\text{C}_6$  system.

The values for  $E_{\text{int}}$  and  $E_{\text{surf}}$  obtained here are supported by trajectory calculations and are also found to depend strongly

(37) Rosenstock, H. M.; Draxl, K.; Steiner, B. W.; Herron, J. T. *Energetics of Gaseous Ions*. *J. Phys. Chem. Ref. Data* **1977**, *6*, Suppl. 1.

(38) Kenttämaa, H. I.; Cooks, R. G. *Int. J. Mass Spectrom. Ion Processes* **1985**, *64*, 79.

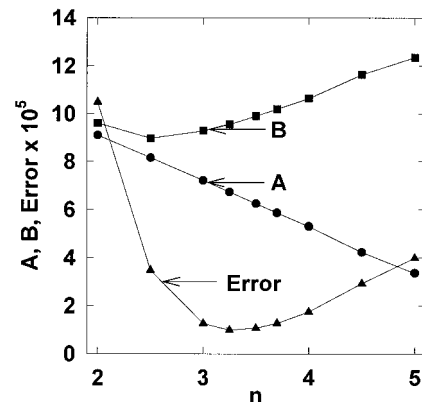


**Figure 5.** Best activation energy  $A$ ,  $B$ , and error values versus  $n$  for fitting the  $\text{SiMe}_3^+ \rightarrow \text{Si}^+$  channel.  $A$  and  $B$  have units of eV while error is unitless.

upon the adsorbate coverage on  $\text{Au}(111)$ ; these results are discussed elsewhere.<sup>33,39</sup> We have used a single value of  $E_{\text{surf}}$  despite the experimental availability of distributions for  $E$  and  $E_{\text{scat}}$  because we can only guess at the distributions for  $E_{\text{int}}$ . The cyclic nature of using  $E_{\text{int}}$  to determine  $E_{\text{surf}}$  to subsequently obtain the activation energies is considered in the Discussion section.

**B. Comparison of Model with Experimental Data.** We have fit our model to the ERMS of the  $\text{SiMe}_2^+$ ,  $\text{SiMe}^+$ ,  $\text{SiD}^+$ , and  $\text{Si}^+$  fragment ions produced as a result of the collision event. These are the higher energy fragment ions produced from SID of  $\text{SiMe}_3^+$ . The  $\text{SiMeD}_2^+$  data were not fit due to insufficient points near the threshold. The fraction of a given fragment ion channel was calculated by numerical integration and then compared with the experimental ERMS by a nonlinear least-squares fit with use of Mathcad (v. 5.0, Mathsoft, Cambridge, MA).  $A$  and  $B$  were varied for a given  $n$  in order to obtain the best fit, as given by comparing the experimental and calculated ERMS for all beam energies  $E_m$  by defining

$$\text{error} = \sum_m [E_m F_i(E_m)_{\text{calc}} - E_m F_i(E_m)_{\text{expt}}]^2 \quad (17)$$

The optimal value of  $n$  was chosen by obtaining the lowest error value for the highest energy fragment of a given mechanism ( $\text{SiD}^+$  and  $\text{Si}^+$ ), and this value of  $n$  was then used for the lower energy fragments formed by that mechanism. The values of  $A$ ,  $B$ , and error as a function of  $n$  are shown in Figure 5 for the formation of the  $\text{Si}^+$  fragment and were also determined for the  $\text{SiD}^+$  fragment (data not shown). It is generally found that the value of  $A$  decreases as a function of  $n$ . The best values of the activation energies  $A$ ,  $B$ , and  $n$  are listed in Table 1 for all of the fragment ions analyzed in this study along with their corresponding literature values.<sup>29,37,40,41</sup>  $A$  and  $B$  have units of eV while error is unitless. The values of  $A$  in Table 1 have been shifted upward by  $1.0 \pm 0.5$  eV compared with those of Figure 5, to account for the initial internal energy of the parent ion (see below). Table 1 also lists the maximum value of  $E(E_{\text{max}})$  for which each fragment ion of the ERMS was fit. The results for the best fits are shown in Figure 6 by plotting both the calculated (curve) and the experimental ERMS (points). The threshold regions of the four fragmentation channels are fit well by the calculated curves. However, consideration of the  $\text{SiMe}_2^+$

(39) Schultz, D. G.; Wainhaus, S. B.; Hanley, L.; de SainteClaire, P.; Hase, W. L. *J. Chem. Phys.* In press.

(40) Lin, C.-Y.; Dunbar, R. C.; Haynes, C. L.; Armentrout, P. B.; Tonner, D. S.; McMahon, T. B. *J. Phys. Chem.* **1996**, *100*, 19659.

(41) Boo, B. H.; Elkind, J. L.; Armentrout, P. B. *J. Am. Chem. Soc.* **1990**, *112*, 2083.

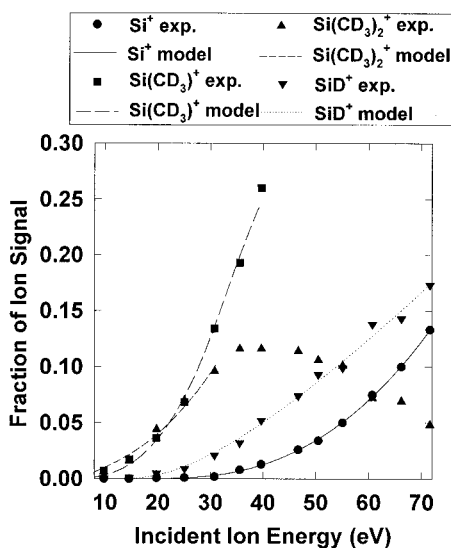


**Figure 6.** Experimental (points) and predicted (curves) ERMS for all four fragment ion channels fit with our model.

**Table 1.** Values of Activation Energies  $A$ ,  $B$ ,  $n$ , and  $E_{\max}$

fragment	method	$n$	$A$ (eV)	$B$ (eV)	$E_{\max}$ (eV)
$\text{Si}(\text{CD}_3)_2^+$	SID <sup>a</sup>	3.25	$4.3 \pm 1.1$	$7.7 \pm 0.6$	30
	CID <sup>b</sup>	$3.0 \pm 0.5$	$5.32 \pm 0.28$		
	EI <sup>c</sup>		7.5		
	EI <sup>d</sup>		3.24		
$\text{Si}(\text{CD}_3)^+$	SID <sup>a</sup>	3.25	$5.6 \pm 1.0$	$4.5 \pm 0.9$	40
	CID <sup>b</sup>	2.5–3.5	$6.58 \pm 0.42$		
	EI <sup>c</sup>		10		
	EI <sup>d</sup>		6.79		
$\text{Si}^+$	SID <sup>a</sup>	3.25	$7.7 \pm 1.1$	$9.6 \pm 1.0$	70
	CID <sup>b,e</sup>	2.1	$10.87 \pm 0.57$		
	EI <sup>c</sup>		11.1		
	EI <sup>d</sup>		7.49		
$\text{SiD}^+$	SID <sup>a</sup>	2.0	$7.5 \pm 1.4$	$14.4 \pm 1.4$	70
	CID <sup>b,e</sup>		$12.2 \pm 0.57$		
	EI <sup>c</sup>				
	EI <sup>d</sup>		7.79		

<sup>a</sup> The  $A$  values from SID (surface-induced dissociation) have been adjusted upward by  $1.0 \pm 0.5$  eV to account for an estimated initial internal energy in  $\text{Si}(\text{CD}_3)_3^+$ . <sup>b</sup> CID = collision-induced dissociation in the gas phase. Reference 40. <sup>c</sup> EI = electron impact. Reference 29. <sup>d</sup> Reference 37. <sup>e</sup> Reference 41.

channel in Figure 6 shows that in its present implementation, our model cannot fit the downturn in the experimental ERMS at higher  $E$  values. Ongoing investigations are using eq 10 to fit the regions of the ERMS above  $E_{\max}$ . The error bars given in Table 1 for the SID values are estimated from the shifts in  $A$  determined at the limits of  $n$  given by the error in the fitting process.

## V. Discussion

The activation energies  $A$ , listed in Table 1 for each of the  $\text{SiMe}_3^+$  fragments, vary over a considerable range. We will estimate the accuracy of our activation energies by comparing them with the CID data.<sup>40,41</sup> It is reasonable to discount the electron impact (EI) data since it is more likely to suffer from nonadiabatic effects, some<sup>37</sup> has not appeared in subsequent compilations of ion thermochemical data,<sup>42</sup> and some<sup>29</sup> was collected primarily to obtain accurate cross-sections rather than activation energies. On the basis of the energy required for the first methyl loss shown in Table 1, the large number of

vibrational modes available to  $\text{SiMe}_3^+$ , and the poor Franck–Condon overlap between  $\text{SiMe}_4$  and  $\text{SiMe}_3^+$ ,<sup>43</sup> it is reasonable to assume that 70-eV EI imparts an initial internal energy to  $\text{SiMe}_3^+$  of  $1.0 \pm 0.5$  eV. Our SID activation energies listed in Table 1 have been corrected by this amount to account for the initial internal energy of the parent ion. The SID activation energies for  $\text{SiMe}_2^+$  and  $\text{SiMe}^+$  are both  $1.0 \pm 1.1$  eV below the CID values. The SID activation energies for  $\text{Si}^+$  and  $\text{SiD}^+$  are  $3.2 \pm 1.2$  and  $4.7 \pm 1.5$  eV below the CID values, respectively.

The offset between the SID and CID  $A$  values results from errors in  $E_{\text{surf}}$ .  $E_{\text{surf}}$  depends on an accurate initial estimation for  $E_{\text{int}}$ ,  $E$ , and  $E_{\text{scat}}$  (eq 15).  $E_{\text{int}}$  has been calculated from a compilation of EI values and was chosen because it includes data for all the methyl loss and rearrangement channels observed in the ERMS.<sup>37</sup> Comparison of the literature  $A$  values in Table 1 indicates that these EI values are probably lower than the correct values. Our use of these EI values to determine  $E_{\text{surf}}$  likely contributes to a significant fraction of the offset in the SID  $A$  values (see above). Simple analysis and trajectory calculations<sup>39</sup> both indicate that the method used to extract  $E_{\text{int}}$  from the ERMS is particularly inaccurate at higher  $E$ ,<sup>23,38</sup> leading to the larger offsets in  $A$  for the  $\text{Si}^+$  and  $\text{SiD}^+$  channels. Future work will attempt to measure this function more carefully. Finally, uncertainties in  $E$  of  $\pm 1$  eV and  $E_{\text{scat}}$  of  $\pm 0.5$  eV also affect  $E_{\text{surf}}$  (see Experimental Section).

The largest uncertainty in fitting ERMS data with this method derives from the choice of  $n$ . Figure 5 clearly shows that for  $\text{Si}^+$ , the values of  $A$  and  $B$  both depend on  $n$ : this is true for all fragment ions. We have chosen the best  $n$  value as that when the error between the model and the data is minimized, which occurs at  $n = 3.25$  for  $\text{Si}^+$  (Figure 5). Since  $\text{Si}^+$  is the highest energy fragment formed by the sequential methyl loss channel and its data set has many points near threshold, we also use its  $n$  value for the lower energy fragments of this channel. Since all the methyl loss fragment ions derive from the same excitation mechanism and our procedure models the excitation step rather than the dissociation step, it is appropriate to use the same  $n$  values here. When fewer points near threshold are available, the minimum in the error vs  $n$  curve may not be as apparent as it is in Figure 5. This makes the  $n$  value uncertain, and this in turn makes the  $A$  value uncertain. Ideally, one should use many points at and near the threshold separated by no more than 1 eV. Since  $\text{SiD}^+$  is formed via a different dissociative channel,<sup>29,36</sup> we repeated the minimization process rather than using the same  $n$  value as for the methyl loss channel.

One major complication in analyzing SID and CID data is the effect on the ERMS of delayed dissociation of the parent ion. Delayed dissociation begins to affect thresholds when the time required for energy randomization and dissociation is longer than the time available for detection ( $\sim 10 \mu\text{s}$  in our experiment). Delayed dissociation is routinely addressed in the deconvolution of CID data by the RRKM method<sup>12,44</sup> and may also need to be taken into consideration for SID. However, delayed dissociation always leads to an overestimation of the activation energies, while the SID  $A$  values reported here are consistently lower than those from CID. The choice of  $n$  can partially take into account the effect of delayed dissociation in that a larger  $n$  shifts  $f_i(E)$  to higher  $E$ . For this reason, it is reasonable that  $n$  either stays the same or decreases from higher to lower energy fragments for a series of sequential dissociations such as methyl loss. Our analysis does not allow  $n$  to be less

(42) Lias, S. G.; Bartmess, J. E.; Liebman, J. F.; Holmes, J. L.; Levin, R. D.; Mallard, W. G. *Gas Phase Ion and Neutral Thermochemistry*. *J. Phys. Chem. Ref. Data* **1988**, *17*, Suppl. No. 1.

(43) McGinnis, S.; Riehl, K.; Haaland, P. D. *Chem. Phys. Lett.* **1995**, *232*, 99.

(44) Loh, S. K.; Hales, D. A.; Lian, L.; Armentrout, P. B. *J. Chem. Phys.* **1989**, *90*, 5466.

than 2 (that is, we do not allow step function behavior). Since methyl loss would be expected to occur on a different time scale than rearrangement, it is reasonable that we have chosen different  $n$  values for these two fragment channels. We suspect that delayed dissociation effects may be smaller for SID than CID due to a forced redistribution of energy in the parent ion internal modes by the complex series of collisions that occur at the surface.

Several factors contribute to uncertainty in the SID activation energies presented here. The uncertainty in the absolute beam energy  $E$  and the energy width of the beam energy  $\Delta E$  are both always  $\geq 1$  eV in any SID experiment, compared with  $\leq 0.3$  eV in a CID experiment.<sup>12,13,44</sup> The higher uncertainty in SID beam energies necessarily results from image charge induced shifts and broadening of the beam energy at the surface, complicated by the possibility that the ion undergoes neutralization and reionization at unknown distances from the surface.<sup>45</sup> While both  $E$  and  $\Delta E$  are measured experimentally, these shift and broadening effects are difficult to quantify and therefore will lead to additional uncertainties both in the experimental ERMS and in the fitting process from which the calculated ERMS is determined. For the  $\text{SiMe}_3^+$  system, the uncertainty in our ERMS leads to an uncertainty in  $n$  of  $\pm 0.75$ , which results in the ca.  $\pm 1$ -eV uncertainty in the SID  $A$  values (Table 1). A separate indeterminate uncertainty in the SID  $A$  values derives from  $E_{\text{surf}}$  (see above).

It can be argued that the method described here is limited by the fact that  $A$  values are used to estimate  $E_{\text{int}}$ , which in turn is used to obtain  $E_{\text{surf}}$ , which in turn leads back to the  $A$  values. There are several solutions to this limitation: (1) An iterative approach can be employed by making an initial guess at  $E_{\text{int}}$ , obtaining  $E_{\text{surf}}$  and  $A$ , using  $A$  to re-estimate  $E_{\text{int}}$ , and then repeating the process until self-consistent values are obtained. This would work for multiple fragmentation channels since they would all use the same  $E_{\text{surf}}$  function. (2) Experimental examination of a sufficient number of ion-surface pairs may provide the ability to predict  $E_{\text{surf}}$  for new systems. (3)  $E_{\text{surf}}$  can be determined in some cases from the parent ion and the first dissociation product, where the  $A$  value is known from another experiment. Then, our procedure would be used for all other fragment ions. (4) Preliminary results have indicated that  $E_{\text{surf}}$  may be obtained from trajectory calculations.<sup>39</sup> A recent analysis of experimental data has found that the  $E_{\text{surf}}$  function is linear with similar slopes and intercepts for several

different ion-surface pairs:<sup>46</sup> this simple behavior in  $E_{\text{surf}}$  adds further credence to the applicability of our method.

The choice of surface composition is vital in obtaining accurate activation energies. If the kinetic to internal energy transfer ( $T-V$ ) is too large, a bunching of thresholds around a similar energy value may occur for all of the fragments, thereby complicating the analysis. Thus, fluorinated organic surfaces<sup>2,3,6,19</sup> and clean Au(111) both show high  $T-V$ <sup>33</sup> and high scattered ion yields, but they may have limited utility for determining activation energies.

## VI. Conclusions

We have demonstrated a new method by which one can obtain activation energies for the formation of fragmentation products of a parent ion during surface-induced dissociation. While this method will probably not exceed the accuracy of gas-phase collision-induced dissociation or other accepted thermochemical methods for small ions, it holds great promise for the larger ions that cannot be readily analyzed by these existing methods. Our method is limited by the ability to determine an accurate function for the transfer of energy to the surface, but this function appears to be relatively well-behaved. Our method is also subject to the same kinetic and internal energy measurement constraints that exist for all thermochemical methods, and these constraints have contributed to uncertainties in the results reported here. However, we are working to reduce these measurement uncertainties through improvement of our experimental apparatus. We are testing our method out on other small polyatomic ions by measuring energy resolved mass spectral data with 1-eV increments in the incident ion energy in the threshold region. This effort is being assisted by trajectory calculations and further theoretical investigations. Once the behavior of a series of smaller ions is well understood, we hope to apply these methods to determine activation energies of high-energy fragmentations of medium to large biological ions, where we hope this method will be most useful.

**Acknowledgment.** This research was funded by the National Science Foundation (CHE-9632517). L.H. is supported by a National Science Foundation Young Investigator Award (1994-98). We would like to thank Hanjo Lim and David Schultz for assistance in collecting the experimental data.

JA962471K

(45) For example, see: Cooper, B. H.; Behringer, E. R. In *Low Energy Ion-Surface Interactions*; Rabalais, J. W., Ed.; Wiley: New York, 1994; p 263.

(46) Hanley, L.; Lim, H. L.; Schultz, D. G.; Wainhaus, S. B.; de SainteClaire, P.; Hase, W. L. *Nucl. Instrum. Methods Phys. Res., Sect. B* In press.